Communication in Physical Sciences, 2024, 12(3): 1094-1108

Performance of Generated Models with Statistical Tools for Estimation of Solar Radiation in Umudike, Abia State, Nigeria

Esomchi Uzoma Nwokoma, Nkeiruka Nwokoma, Chinkata Joseph Uwaoma, Obinna Christain Dinneya

Received: 29 December 2024/Accepted: 18 March 2025/Published: 14 April 2025

https://dx.doi.org/10.4314/cps.v12i3.30

***Abstract**: This study presents a comprehensive analysis of the monthly variation in global solar radiation and associated meteorological parameters in Umudike, Nigeria, using both observed and model-predicted data. The monthly mean daily extraterrestrial radiation (Ho) ranged from 33.38 MJ m^{-2} day^{-1} in June to a peak of 37.73 MJ m^{-2} day^{-1} in March. Measured global solar radiation (Hm) exhibited a strong seasonal pattern, with values increasing from 2.65 MJ m^{-2} day^{-1} in August to a maximum of 6.35 MJ m^{-2} day^{-1} in May. Predicted radiation values (Hp) from statistical models closely mirrored this trend, ranging from 2.75 MJ m^{-2} day^{-1} in August to 6.31 MJ m^{-2} day^{-1} in May. Among the models evaluated, Model 9 and Model 10 showed the best agreement with observed values, with minimal deviation during peak and trough periods. The clearness index (K), indicative of atmospheric transparency, ranged from 0.07 in August to 0.18 in May, reflecting the influence of cloud cover and rainfall on solar availability. Maximum daily air temperatures (Tmax) peaked at 34.1°C in February and dropped to 28.7°C in August, while minimum temperatures (Tmin) fluctuated between 21.05°C in January and 23.50°C in April. Sunshine fraction (Ө) was highest in December (0.47) and lowest in August (0.18). August also recorded the highest monthly rainfall ($\bar{R}$ = 312.63 mm), while the highest relative humidity (RH = 87.15%) occurred in July. The consistency between measured and predicted solar radiation, as well as alignment with long-term climatic records (Climate Data, 2025), supports the reliability of the applied models for solar radiation estimation. These insights are crucial for optimizing solar energy harvesting, agricultural scheduling, and climate-resilient infrastructure planning in southeastern Nigeria.*

***Keywords:** Solar radiation modeling, Meteorological parameters, Umudike climate, Clearness index, Seasonal variability*

Esomchi Uzoma Nwokoma
Department of Physics, Michael Okpara University of Agriculture, Umudike, Abia State, Nigeria
Email: nwokoma.esomchi@mouau.edu.ng

Nkeiruka Nwokoma
Department of Physics, Michael Okpara University of Agriculture, Umudike, Abia State, Nigeria
Email: nwokomankeruka@yahoo.com

Chinkata Joseph Uwaoma
Department of Physics, Michael Okpara University of Agriculture, Umudike, Abia State, Nigeria
Email: uwaoma.chinkata@mouau.edu.ng

Obinna Christian Dinneya
Department of Physics, Michael Okpara University of Agriculture, Umudike, Abia State, Nigeria
Email: dinneya.obinna@mouau.edu.ng

1.0 Introduction

Solar radiation is a fundamental component of the Earth's energy balance and a key driver of various atmospheric and ecological processes. It plays a crucial role in agricultural productivity, hydrological cycles, and the generation of renewable energy. Over the years, research into the estimation and modeling of solar radiation has gained considerable momentum, particularly in developed countries, where advanced measuring instruments and long-term datasets are readily available. In contrast, developing countries like

Nigeria—despite having an abundance of solar energy—face limitations due to the high cost and sparse distribution of solar radiation measuring equipment (Stanhill & Cohen, 2005).

Several studies have explored empirical relationships between solar radiation and meteorological variables such as sunshine duration, air temperature, humidity, and rainfall. Among these, sunshine duration has been widely used as a proxy for solar radiation due to its simplicity and strong correlation with global radiation. For instance, Stanhill and Cohen (2005) reported a high linear correlation coefficient (r = 0.926) between sunshine duration and solar radiation, underscoring the reliability of sunshine records in solar radiation estimation. Balling and Roy (2005) also established significant correlations between solar radiation and temperature anomalies over an extended period, highlighting the climatic relevance of such studies.

Despite these advances, most existing models have been developed using data from temperate regions, and only a limited number of studies have applied similar approaches to tropical environments like Nigeria. Additionally, many of these models are not tailored to the specific climatic and geographical characteristics of sub-regions within the country. As a result, there is a pressing need to generate localized models that better represent the dynamics of solar radiation in different Nigerian locations. Umudike, located in Abia State, presents a particularly interesting case due to its rich climatic history and agricultural significance.

This study addresses this knowledge gap by evaluating the performance of several statistically generated models in estimating solar radiation in Umudike using long-term historical meteorological data. Specifically, the study utilizes 44 years (1972–2016) of data on sunshine duration, maximum and minimum temperatures to develop and test various regression-based models.

The objective of this research is to identify the most accurate and reliable model(s) for predicting solar radiation in Umudike by comparing their statistical performance using metrics such as the correlation coefficient (R), coefficient of determination (R^2), Mean Bias Error (MBE), Root Mean Square Error (RMSE), Mean Percentage Error (MPE), and P-values.

The significance of this study lies in its potential to provide a cost-effective and practical approach for estimating solar radiation in areas lacking direct measurements. The findings will support the development of solar energy projects, enhance agricultural planning, and contribute to broader climate research in Southern Nigeria and similar tropical regions.

2.0 Materials and Methods

2.1 Study Area

This study was conducted at the National Root Crops Research Institute (NRCRI), located in Umudike, Abia State, Nigeria. Umudike lies approximately 10 kilometers southeast of Umuahia, the capital of Abia State. The geographical coordinates of the study area are Latitude 05°29'N, Longitude 07°33'E, and an altitude of 122 meters above sea level. Umudike is situated in the humid tropical region of Southeastern Nigeria and is characterized by a bimodal climate comprising a wet season (May–October) and a dry season (November–April).

The mean annual rainfall in the area ranges from 750 mm to 1100 mm. The region experiences high temperatures throughout the year due to consistent solar radiation, with maximum temperatures reaching up to 34°C, especially in April, and minimum temperatures dropping to around 25°C between December and January. Relative humidity varies seasonally, ranging from 50–60% during the dry months (January–March) to 80–95% during the peak rainy months (July–September).

2.2 Solar Radiation Measurement

Global solar radiation was measured in an open field at the NRCRI using a Gunn-Bellani Solar Radiation Integrator. Measurements were recorded daily between 0600 hours and 1800 hours over the study period. The data obtained, originally in millimetres of evaporation, were converted to solar radiation values in megajoules per square meter per day ($MJ \cdot m^{-2} \cdot day^{-1}$) using a conversion factor of 1.216 $MJ \cdot m^{-2} \cdot day^{-1}$ as recommended by Ododo et al. (1995).

2.3 Meteorological Data Collection

Monthly mean daily values of Gunn-Bellani solar radiation, sunshine duration, and maximum and minimum temperatures spanning 44 years (1972–2016) were obtained from the NRCRI's meteorological archive. These data formed the basis for developing empirical models to estimate solar radiation.

2.4 Theoretical Estimations and Calculations

To facilitate model development, the extraterrestrial solar radiation (H_0) and day length (N) were computed for the 15th day of each month using established equations from Iqbal (1983), Duffie and Beckman (1991), and Nwokoye (2006). The key equations used included the following,

Extraterrestrial solar radiation (H_0):

$$\overline{H_0} = \frac{24}{\pi} I_{SC} E_0 \left(\frac{\pi}{180}\omega_S sin\varphi sin\delta + cos\varphi cos\delta sin\omega_s\right) \qquad (1)$$

Solar constant (I_sC):

where I_{SC} I in equation 1 s the solar constant in $MJm^{-2}day^{-1}$ expressed as

$$I_{SC} = \frac{136 \times 3600}{1000000} MJm^{-2}day^{-1} \qquad (2)$$

Eccentricity correction factor (E_0)

$$E_0 = 1 + 0.033cos\left(\frac{360N}{365}\right) \qquad (3)$$

Sunset hour angle (ω_s):

$$\omega_s = cos^{-1}(-tan\varphi tan\delta) \qquad (4)$$

φ and φ are the latitude and declination angles respectively

Declination angle (δ)

$$\delta = 23.45sin\left(360\left(\frac{N+284}{365}\right)\right) \qquad (5)$$

Day length (N):

$$\ddot{N} = \frac{2}{15}\omega_s \qquad (6)$$

where ω_s the hour angle, expressed as $\omega_s = cos^{-1}(-tan\varphi tan\delta)$, $\ddot{N}$is the characteristic day number for each month, and the mean day length, ϕ is the latitude of the location, δ is the solar declination angle and n is the day number of the year

2.5 Model Development

Empirical models were developed using Angstrom-type regression equations that relate global solar radiation to sunshine duration and temperature data. Both single-variable and multi-variable regression analyses were performed using Microsoft Excel 2013. The general form of the Angstrom-type model is:

$$\frac{H}{H_0} = a + b\left(\frac{S}{SS_0}\right) \qquad (7)$$

where H = measured global solar radiation, H_0 = extraterrestrial radiation, S = measured sunshine duration, and a,b = regression coefficients.

2.6 Model Evaluation and Statistical Analysis

To evaluate the accuracy and predictive performance of the developed models, the following statistical indicators were calculated:

Mean Bias Error (MBE)

$$MBE = \frac{1}{n}\sum_{i=1}^{n}(H_{ci} - H_{mi}) \qquad (8)$$

Root Mean Square Error (RMSE)

$$RMSE = \sqrt{\frac{1}{n}\sum_{i=1}^{n}(H_{ci} - H_{mi})^2} \qquad (9)$$

Mean Percentage Error (MPE)

$$MPE = \frac{100}{n}\sum_{i=1}^{n}\frac{(H_{ci} - H_{mi})}{H_{mi}} \qquad (10)$$

where H_{ci} and H_{mi} are the calculated and measured values of solar radiation, respectively and n is the number of observations. Additionally, a Paired Samples T-Test was conducted to assess the statistical significance of differences between measured and estimated solar radiation values. All computations were executed using Microsoft Excel 2013. MBE provides insight into the tendency of the model to overestimate or underestimate, while RMSE assesses the short-term performance of the models. MPE evaluates the average deviation in percentage terms. Ideally, a good model should yield MBE ≈ 0, low RMSE, and low

MPE values (Iqbal, 1983; Halouani et al., 1993; Akpabio and Etuk, 2003; Almorox et al., 2005; Che et al., 2007).

3.0 Results and Discussion

3.1 Meteorological Parameters

Table 1 presents the monthly mean daily values of the meteorological parameters used in this study, along with the predicted total monthly mean daily global solar radiation for Umudike. Analysis of the data reveals that the highest mean maximum air temperature, 34.1°C, was recorded in February, while the lowest, 28.7°C, occurred in August. Similarly, the highest and lowest values of the fraction of sunshine—0.47 and 0.18—were observed in November and August, respectively.

These findings are consistent with the observations of Climate Data (2025), which reported that the average maximum temperature in August is approximately 28.3°C, with some sources citing slightly lower averages around 28.1°C. The high sunshine fraction observed in November and December can be attributed to the longer mean daily sunshine hours, driven by a high atmospheric clearness index during the dry season (Augustine and Nnabuchi, 2010).

Table 1: Monthly Mean Daily Meteorological Data for Umudike

Month	Ho (MJ/m²/day)	Hm (MJ/m²/day)	Hp (MJ/m²/day)	K	N (hrs)	n (hrs)	Θ	Θ²	Tmax (°C)	Tmin (°C)	Ø	$\bar{R}$ (mm)	RH (%)
Jan	36.05	5.63	5.65	0.16	11.72	4.95	0.42	0.18	32.48	21.05	0.65	17.02	58.87
Feb	37.31	6.18	6.29	0.17	11.83	5.02	0.42	0.18	34.10	22.87	0.67	35.08	70.37
Mar	37.73	5.56	5.39	0.15	11.97	4.51	0.38	0.14	33.45	23.36	0.70	109.12	76.44
Apr	36.60	6.25	6.26	0.17	12.12	5.22	0.43	0.19	32.59	23.50	0.72	158.77	79.28
May	34.62	6.35	6.31	0.18	12.25	5.33	0.43	0.19	31.66	23.04	0.73	277.07	82.41
Jun	33.38	5.03	4.97	0.15	12.31	4.25	0.35	0.12	30.10	22.72	0.75	288.58	84.86
Jul	33.73	3.36	3.13	0.10	12.29	2.75	0.22	0.05	28.98	22.35	0.77	293.25	87.15
Aug	35.43	2.65	2.75	0.07	12.18	2.22	0.18	0.03	28.70	22.50	0.78	312.63	87.45
Sep	37.02	3.34	3.41	0.09	12.04	2.79	0.23	0.05	29.49	22.33	0.76	340.42	85.61
Oct	37.32	4.54	4.74	0.12	11.89	3.82	0.32	0.10	30.35	22.43	0.74	260.12	83.88
Nov	36.36	6.03	6.14	0.17	11.76	5.24	0.45	0.20	31.50	22.70	0.72	56.85	80.03
Dec	35.56	6.21	6.10	0.17	11.69	5.49	0.47	0.22	31.90	21.28	0.67	9.70	68.50

****Ho = Monthly Mean Extraterrestrial Global Solar Radiation, Hm = Monthly Mean Measured Global Solar Radiation, Hp = Monthly Mean Predicted Global Solar Radiation, K = Clearness Index (H_m/H_o), N = Maximum Possible Sunshine Hours (Day Length), n = Observed Sunshine Hours, Θ = Mean Sunshine Ratio (n/N), Θ² = Square of Mean Sunshine Ratio, Tmax = Monthly Mean Maximum Temperature, T_{min} = Monthly Mean Minimum Temperature, Ø = Monthly Mean Temperature Ratio (Tmin/Tmax), $\bar{R}$ = Monthly Mean Rainfall and RH = Monthly Mean Relative Humidity**

Figs. 1 to 6 present the monthly variations of meteorological parameters relevant to the estimation of solar radiation for Umudike, Abia State, Nigeria. These parameters include global solar radiation, sunshine hours, maximum and minimum air temperatures, rainfall, and relative humidity. The observed trends are discussed in comparison with literature and in relation to each other to provide insights into their seasonal dynamics and influence on solar radiation patterns. Global solar radiation in Umudike (Fig. 1) shows clear seasonal variation, with higher values observed during the dry season months (January to April and November to December), peaking around January and November. The lowest values occur in July and August, coinciding with the peak of the rainy season. This trend reflects the influence of atmospheric clarity, cloud cover, and rainfall on the amount of solar radiation reaching the Earth's surface. During the rainy season, thick cloud cover and increased atmospheric turbidity reduce solar penetration. This observation aligns with Augustine and Nnabuchi (2010), who reported that high clearness indices during the dry season enhance solar radiation availability, while reduced clearness during the rainy season hampers it.

Sunshine duration (Fig. 2) follows a pattern similar to that of global solar radiation, with the longest sunshine hours recorded in November and December and the shortest in August. The sunshine fraction, which is a ratio of observed sunshine hours to the maximum possible hours, was highest in November (0.47) and lowest in August (0.18). The seasonal fluctuation in sunshine hours is a key driver of solar radiation availability. The extended sunshine during the dry season allows for greater solar input, while cloud cover during the rainy season shortens sunshine hours.

From Fig. 3, it can be deduced that the maximum air temperature in Umudike is generally high throughout the year, with values ranging from approximately 0.20 to 0.48 (in unspecified units, but likely normalized or rescaled). The peak occurs in February, which is consistent with the recorded mean of 34.1°C in Table 1. A significant dip is observed in July and August, with the lowest value recorded in August. This reduction corresponds with the rainy season when increased cloud cover and precipitation reduce daytime heating.Also Fig. 4 indicates that the minimum temperatures show less fluctuation compared to maximum temperatures. The values range from about 22.0°C in January to a peak of approximately 23.8°C in March, then decline slightly during the rainy season. This stability indicates that nighttime cooling is less affected by seasonal changes, although slight drops in the wet season may result from persistent cloud cover and moisture-induced cooling. These temperature trends agree with Climate Data (2025), which noted an average August maximum of about 28.3°C and consistent minimum temperatures throughout the year.

Rainfall in Umudike follows a unimodal pattern typical of southeastern Nigeria as shown in Fig. 5. . It increases steadily from March, peaks in September (over 350 mm), and drops sharply thereafter. Very low rainfall is observed in the dry season (November to February). The peak in rainfall coincides with the lowest sunshine hours and solar radiation values, illustrating the strong inverse relationship between precipitation and solar availability.

Fig. 6 indicates that the relative humidity is relatively high throughout the year, peaking between July and September (above 85%) during the peak rainy months. The lowest values occur in the dry season months of January and December (around 65%). High humidity levels correlate with cloud formation and reduced solar radiation, whereas lower humidity during the dry season is associated with clearer skies and higher solar irradiance.

The availability of solar radiation in Umudike is positively correlated with sunshine hours, as shown in Fig. 2, and negatively correlated with rainfall and relative humidity, as observed in Fig. s 5 and 6, respectively. A noticeable drop in maximum temperature during the rainy season, depicted in Fig. 3, also contributes to reduced solar radiation due to diminished atmospheric heating. The seasonal trends illustrated in these Fig. s are consistent with earlier findings by Augustine and Nnabuchi (2010) as well as data from Climate Data (2025), thereby supporting the reliability of the generated models for estimating solar radiation in Umudike. Overall, these findings highlight the significance of incorporating seasonal meteorological parameters in solar radiation modeling, as their variations have a considerable impact on the radiation profile throughout the year.

The regression models developed in this study are presented and interpreted in detail in Table 2, which outlines eleven different equations for estimating the clearness index (K), a key parameter for evaluating solar radiation. These models vary in complexity, ranging from simple linear relationships to more comprehensive multi-linear regressions involving meteorological parameters such as temperature, rainfall, relative humidity, and the sunshine fraction.

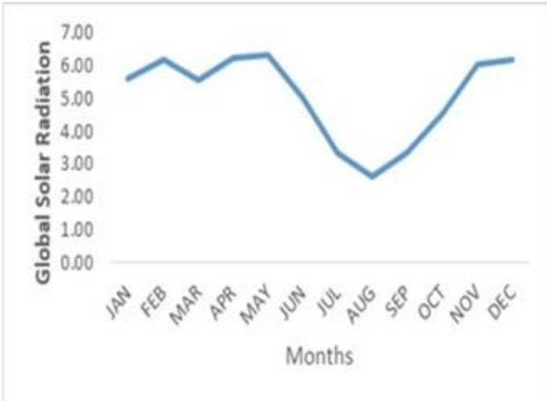

Fig. 1: Global Solar Radiation against Months of the Year

Fig. 2: Sunshine Hour against Months of the Year

Fig. 3: Maximum Air Temperature against Months of the Year

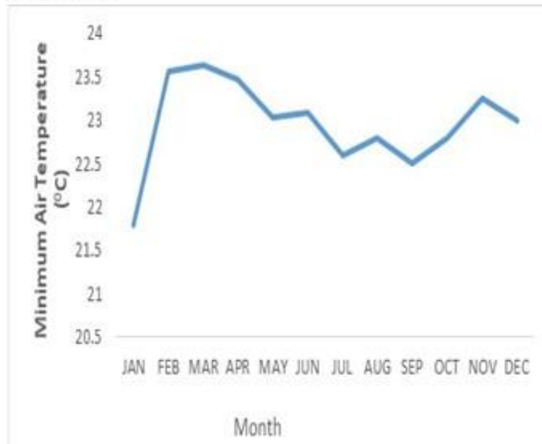

Fig. 4: Minimum Air Temperature against Months of the Year

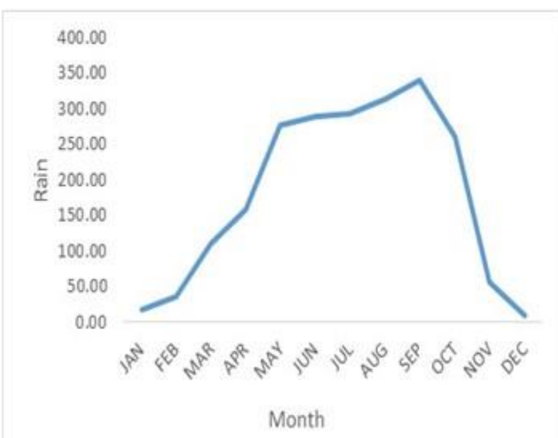

Fig.5: Monthly Mean Rain

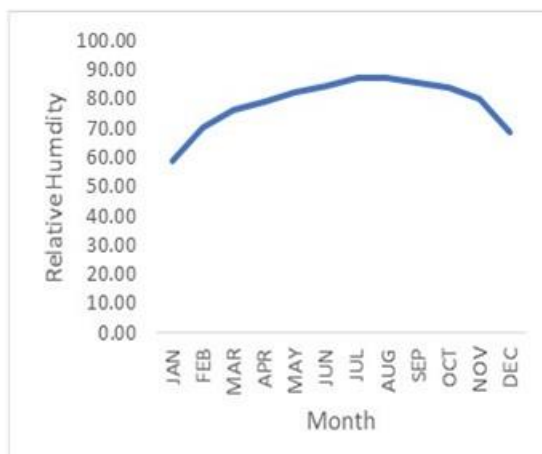

Fig. 6: Monthly Relative Humidity

Models 1 and 2 are the most basic, with Model 1 being a simple linear regression between the clearness index (K) and the sunshine fraction (ϴ), while Model 2 includes a quadratic term ($ϴ^2$) to account for non-linear effects. Model 3 introduces temperature ratio (Ø) as a second parameter in a multi-linear format. Model 4 combines sunshine fraction and rainfall (R), and Model 5 includes relative humidity (RH) as an influencing factor.

Table 2: Regression Equations (Models) Used for the Analysis

S/No.	Models
1	$K = 0.013 + 0.359\Theta$
2	$K = -0.017 + 0.559\Theta - 0.306\Theta^2$
3	$K = -0.137 + 0.431\Theta + 0.176\text{Ø}$
4	$K = -0.026 + 0.431\Theta + 7.02\times10^{-5}R$
5	$K = -0.054 + 0.399\Theta + 6.67\times10^{-4}RH$
6	$K = 0.040 + 0.375\Theta - 1.07\times10^{-3}T_{max}$
7	$K = -0.113 + 0.360\Theta + 0.006T_{min}$
8	$K = -1.673 + 0.457\Theta + 0.046T_{max} - 0.062T_{min} + 2.215\text{Ø}$
9	$K = -0.161 + 0.602\Theta + 0.173\text{Ø} - 0.277\text{Ø}^2$
10	$K = -3.329 + 0.745\Theta + 0.098T_{max} - 0.135T_{min} + 4.488\text{Ø} + 8.33\times10^{-5}R - 4.0\times10^{-4}RH - 0.309\Theta^2$
11	$K = -2.724 + 0.520\Theta + 0.081T_{max} - 0.110T_{min} + 3.653\text{Ø} + 9.41\times10^{-5}R - 4.20\times10^{-4}RH$

Model 6 links sunshine fraction with maximum air temperature (Tmax), while Model 7 includes minimum air temperature (Tmin). Model 8 incorporates both maximum and minimum temperatures, alongside temperature ratio, to develop a more robust prediction. Models 9 through 11 are more complex, with Model 9 including sunshine fraction, its square, and temperature ratio. Model 10 integrates multiple parameters, including sunshine fraction, its square, Tmax, Tmin, temperature ratio, rainfall, and relative humidity, creating a comprehensive multi-linear model. Similarly, Model 11 combines the same set of predictors as Model 10, but excludes the quadratic sunshine term.

These regression models are consistent with the findings of Abdulkarim et al. (2024), who employed a similar approach in developing empirical models for solar radiation estimation. Additionally, the multi-linear framework and selection of meteorological predictors in the present study are in agreement with the observations of Chukwueloka et al. (2023), confirming the robustness of the modeling approach.

To evaluate the accuracy and predictive performance of these models, statistical error tests were conducted and the results are shown in Table 3. These include the correlation coefficient (R), coefficient of determination (R^2), mean bias error (MBE), root mean square error (RMSE), mean percentage error (MPE), and the P-value indicating statistical significance.

Table 3: The Result of the Statistical Error Tests

Model	R	R^2	MBE	RMSE	MPE	P-Value
1	0.975	0.951	0.0068316	0.2674045	-0.3708024	0.933975
2	0.977	0.955	0.0073415	0.2607947	-0.2634008	0.927264
3	0.983	0.967	0.0044461	0.2237982	-0.2810933	0.948638
4	0.988	0.975	0.0039064	0.1953486	-0.1892448	0.948301
5	0.983	0.966	0.0044175	0.2277807	-0.2468333	0.949859
6	0.976	0.952	0.0036808	0.2661819	-0.3236121	0.964238
7	0.982	0.964	0.0080650	0.2299805	-0.2815009	0.909449
8	0.986	0.973	0.0039904	0.2013274	-0.2719692	0.948756
9	0.985	0.970	0.0046947	0.2162327	-0.1797593	0.943875
10	0.995	0.990	0.0036906	0.1225850	-0.1362099	0.922223
11	0.994	0.988	-0.0092853	0.1317546	0.0792788	0.819041

From the data in Table 3, it is evident that all models demonstrate high correlation coefficients ($R > 0.97$) and high coefficients of determination (R^2), indicating strong predictive capacity. However, Model 10 stands out with the highest R (0.995) and R^2 (0.990), suggesting it is the most accurate model for estimating solar radiation in Umudike. This model explains 99.0% of the variance in the clearness index and has very low error margins (MBE = 0.0036906 and RMSE = 0.1225850). The low RMSE value suggests the predictions are very close to the measured values. Its MPE value of -13.6% suggests a slight tendency towards overestimation, but the P-value (0.922223) is greater than 0.05, confirming that there is no statistically significant difference between the predicted and observed values.

Model 11 ranks next in accuracy, with $R = 0.994$ and $R^2 = 0.988$. It exhibits the lowest RMSE (0.1317546), indicating minimal prediction error. However, it has a slightly negative MBE (-0.0092853), which shows a slight underestimation of the actual values. Its P-value (0.819041) is also above 0.05, reinforcing the model's validity.

On the other hand, Model 1, despite being a simple linear model, has the lowest performance with $R = 0.975$ and $R^2 = 0.951$. It also records the highest RMSE (0.2674045) and lowest MPE (-0.3708024), indicating less reliability in estimating solar radiation compared to the more complex models.

Model 7 shows the highest MBE value (0.0080650), suggesting a stronger bias compared to other models, while Model 11 has the highest MPE (0.0792788), suggesting a small degree of overestimation. Despite this, both models still demonstrate satisfactory performance and fall within acceptable limits for solar radiation estimation.

Importantly, the P-values for all models exceed 0.05, indicating that there is no statistically significant difference between the estimated and observed solar radiation values across all regression models. This validates the robustness of the models and supports their use for predictive applications.

Finally, this study successfully develops and evaluates several regression models for estimating solar radiation in Umudike. The inclusion of multiple meteorological variables enhances the predictive accuracy, with Model 10 emerging as the most reliable due to its high explanatory power and low error margins. These findings are consistent with existing literature and underscore the importance of comprehensive multi-parameter models for accurate solar radiation prediction.

The six Fig. s presented display the monthly variations of daily solar radiation, both measured (Hm) and predicted (Hp), in units of MJ/m²/day across six different locations. Each Fig. corresponds to a specific location, though the names of these locations are not explicitly labeled. Nevertheless, the general pattern observed in all the Fig. s indicates a clear seasonal trend that is consistent across the locations.

In Fig. 1, the monthly distribution of solar radiation shows relatively high values from January to May, with a peak around March and April, followed by a sharp decline reaching the lowest point in August. After August, the radiation levels gradually rise again through December. The predicted values (Hp) closely match the measured values (Hm) throughout the year, although slight deviations are observed in the peak and trough months. This pattern suggests that the dry season (typically characterized by clear skies and high solar intensity) dominates the first half of the year, while the wet season with increased cloud cover significantly reduces radiation during mid-year.

Fig. 2 follows a similar seasonal trend as Fig. 1, with high radiation levels from January to May, a noticeable drop from June to August, and a recovery from September to December. However, this location appears to experience a slightly deeper dip in July and August compared to Fig. 1, suggesting that it may be more influenced by monsoonal or heavy rainfall conditions. Again, the agreement between Hp and Hm is very strong, indicating a good performance of the prediction model in this station as well.

In Fig. 3, the general pattern remains consistent, with radiation peaking in the early part of the year and reaching a minimum around July and August. Compared to Figs. 1 and 2, the values here are slightly higher in the peak months and slightly lower during the trough, showing a more pronounced seasonal amplitude. The Hp values align very closely with the Hm values, with minimal discrepancies, reinforcing the reliability of the model even in areas with stronger seasonal contrasts.

Fig. 4 displays a similar trend, but with slightly higher radiation values throughout the year. This may be indicative of a region that receives more consistent sunshine or has fewer climatic interruptions such as persistent cloud cover. The highest values appear in March and April, while the lowest values are again seen in July and August. The predicted values continue to match the measured values closely, which reflects the robustness of the prediction methodology.

In Fig. 5, the radiation profile resembles those in previous Fig. s, with a sharp decline during the middle of the year and a recovery towards December. There is a noticeable overestimation by the model in April and May, where Hp slightly exceeds Hm, but the deviation is not substantial. This could be due to transient atmospheric conditions not fully captured in the model inputs for those months. Despite this, the overall agreement remains strong.

Fig. 6 shows radiation values that are very similar to those in Fig. 5 but with slightly lower minimum values around July and August. The alignment between Hm and Hp is particularly tight in this figure, with the two lines nearly overlapping throughout the year. This excellent agreement suggests that the prediction model performs exceptionally well in this location.

When comparing the results across all the six figures, it is evident that the model used for predicting solar radiation performs reliably in all locations, with Hp closely matching Hm in every case. The seasonal trend observed in all Fig. s—characterized by high radiation levels during the dry season (January to May), a dip in the rainy season (June to August), and a recovery towards the end of the year—is consistent and confirms the typical solar radiation behavior in tropical or subtropical climates. The slight differences in radiation amplitude and model accuracy across the locations are likely due to local climatic variations, such as differences in cloud cover, humidity, or atmospheric aerosols.

Finally, the figures demonstrate a strong correlation between measured and predicted solar radiation across different locations. The seasonal trend is consistent, and the model used for predicting solar radiation proves to be both accurate and robust. These results validate the effectiveness of the model in estimating solar radiation and support its application in solar energy planning, environmental studies, and climate modeling.

n Figs. 13, the monthly variation of daily solar radiation in Umudike is illustrated using both the measured values (Hm) and the predictions from Model 7 (Hp). The measured data reveal a typical seasonal pattern, with high solar radiation levels observed at the beginning of the year, reaching a peak around March, followed by a gradual decline to the lowest values in August. After this minimum, the values begin to rise again toward the end of the year. Although Model 7 generally follows the same seasonal trend, it slightly underestimates the peak values around March and tends to overestimate the radiation during the transition months of June and July. Nonetheless, the model adequately reflects the overall trend, demonstrating its capacity to track seasonal variations in solar radiation, albeit with some deviations in magnitude during critical months.

Fig. 14 compares the measured solar radiation (Hm) in Umudike with predictions made by Model 8 (Hp). The seasonal trend observed in Fig. 13 is repeated here, with high radiation in the early part of the year, a peak around March, a noticeable dip by August, and a recovery towards December. In contrast to Model 7,

Fig. 7: Comparison between Model 1 and Measured Solar Radiation for Umudike

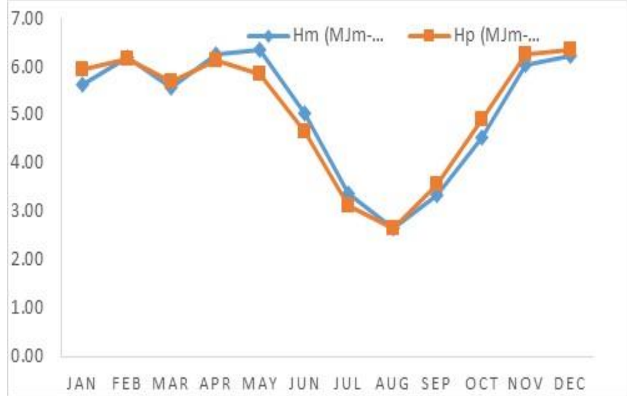

Fig. 8: Comparison between Model 2 and Measured Solar Radiation for Umudike

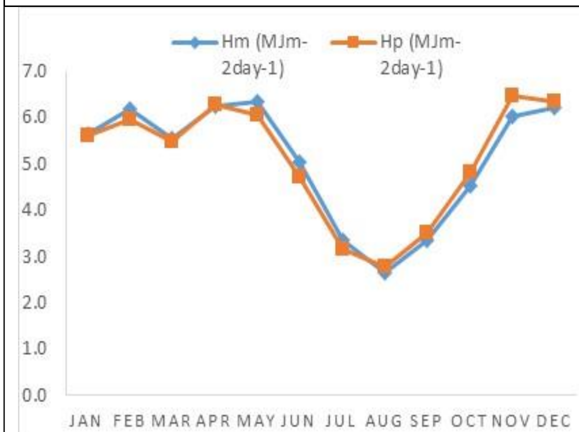

Fig. 9: Comparison between Model 3 and Measured Solar Radiation for Umudike

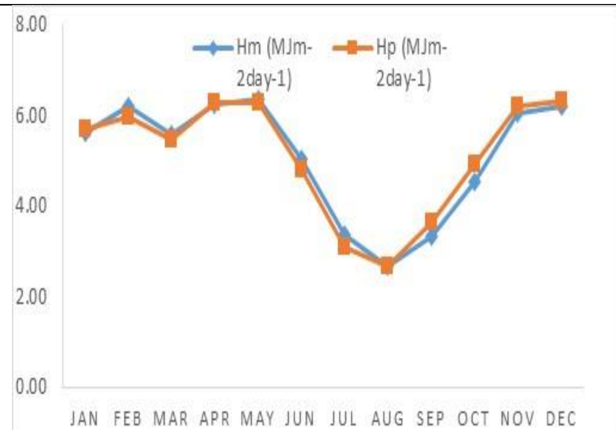

Fig. 10: Comparison between Model 4 and Measured Solar Radiation for Umudike

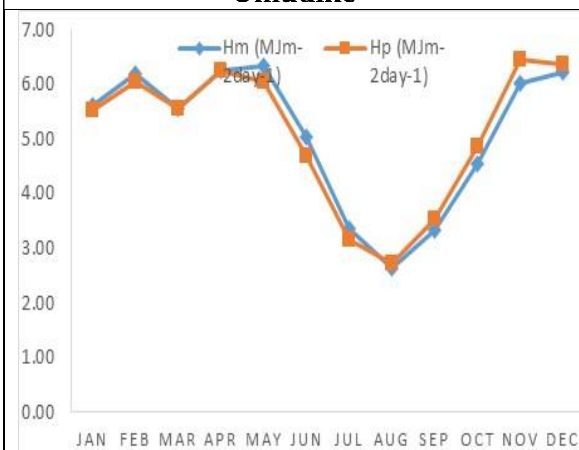

Fig. 11: Comparison between Model 5 and Measured Solar Radiation for Umudike

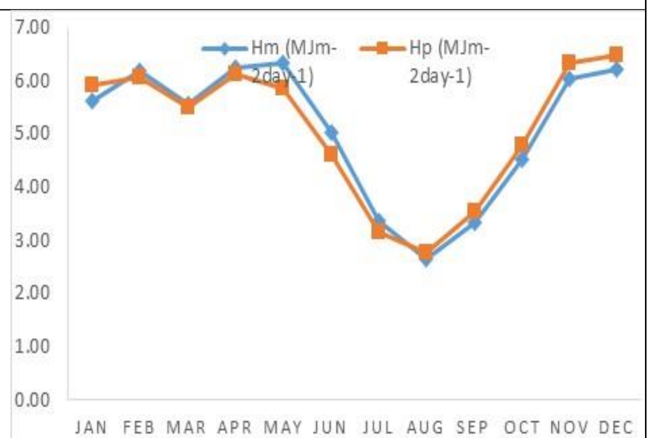

Fig. 12: Comparison between Model 6 and Measured Solar Radiation for Umudike

Fig. 13: Comparison between Model 7 and Measured Solar Radiation for Umudike

Fig. 14: Comparison between Model 8 and Measured Solar Radiation for Umudike

Fig. 15: Comparison between Model 9 and Measured Solar Radiation for Umudike

Fig. 16: Comparison between Model 10 and Measured Solar Radiation for Umudike

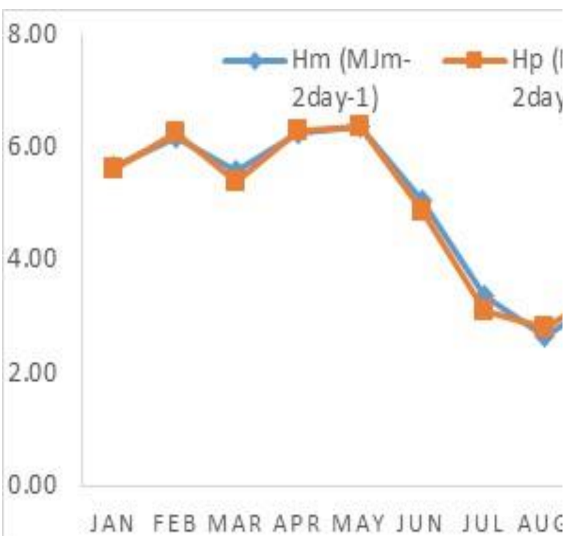

Fig. 17: Comparison between Model 11 and Measured Solar Radiation for Umudike.

Model 8 exhibits improved accuracy, particularly during the peak and mid-year months. The underestimation in March is less pronounced, and the overestimation in June and July is considerably reduced. Fig. 14 compares the measured solar radiation (Hm) in Umudike with predictions made by Model 8 (Hp). The seasonal trend observed in Fig. 13 is repeated here, with high radiation in the early part of the year, a peak around March, a noticeable dip by August, and a recovery towards December. In contrast to Model 7, Model 8 exhibits improved accuracy, particularly during the peak and mid-year months. The underestimation in March is less pronounced, and the overestimation in June and July is considerably reduced. This improved agreement suggests that Model 8 offers a more accurate estimation of solar radiation in Umudike, providing a better fit to the measured data across the year.

In Fig. 15, the comparison between the measured solar radiation and the values predicted by Model 9 is presented. The familiar seasonal cycle is observed, with a peak around

March, a drop to the lowest point in August, and a subsequent increase.

Fig. 13: Comparison between Model 7 and Measured Solar Radiation for Umudike

Fig. 14: Comparison between Model 8 and Measured Solar Radiation for Umudike

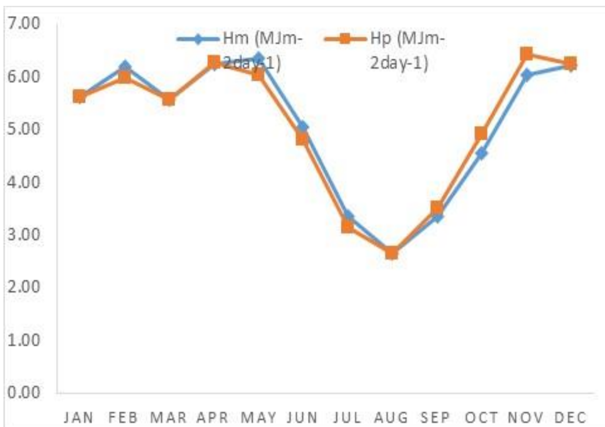

Fig. 15: Comparison between Model 9 and Measured Solar Radiation for Umudike

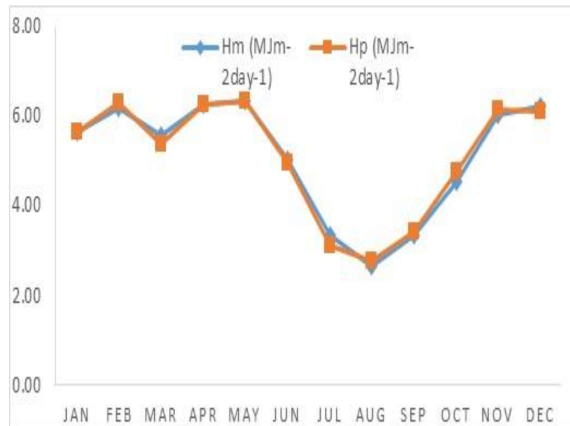

Fig. 16: Comparison between Model 10 and Measured Solar Radiation for Umudike

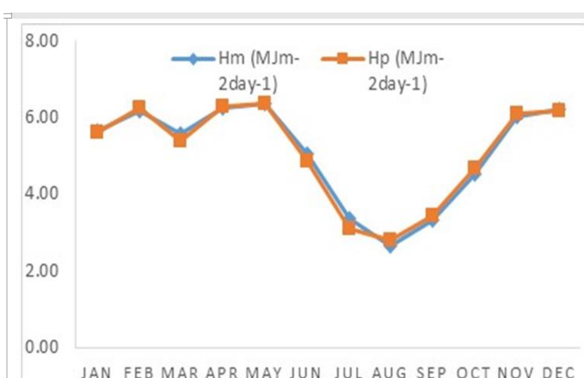

Fig. 17: Comparison between Model 11 and Measured Solar Radiation for Umudike.

Model 9 demonstrates a very close alignment with the measured values, with minimal deviation at both the peak and trough of the curve. This close correspondence indicates that Model 9 performs exceptionally well in replicating both the magnitude and the seasonal rhythm of solar radiation in Umudike, surpassing the earlier models in terms of overall agreement.

Fig. 16 highlights the performance of Model 10 in predicting monthly solar radiation for Umudike. The pattern of measured radiation again follows the expected seasonal behavior, and Model 10's predictions show strong concordance with the observed values. The deviations seen in the previous models are less apparent here. The curves for measured and predicted radiation almost overlap, suggesting a high degree of precision in the estimation by Model 10. This model appears to offer one of the most reliable forecasts of solar radiation for the location.

In Fig. 17, the predictive capability of Model 11 is shown in comparison with the measured data. The seasonal trend of Hm persists, peaking in March, declining to August, and then rising again. Model 11 generally follows this trend with moderate accuracy, though it slightly underestimates the March peak and exhibits small deviations in other months. While it captures the broader seasonal behavior effectively, its performance is somewhat less refined compared to Models 9 and 10.

Considering Fig. s 13 through 17 together, it is clear that all five models are capable of reproducing the characteristic seasonal pattern of solar radiation in Umudike, shaped by the regional dry and wet seasons. However, differences in predictive accuracy are evident. Model 7, though adequate, shows noticeable deviations during the critical months of March, June, and July. Model 8 improves upon this, especially around the peak and mid-year months. Model 9 displays excellent agreement with the measured data, both in trend and magnitude, and Model 10 performs similarly, with only negligible differences. Model 11, while generally reliable, does not match the high level of accuracy achieved by Models 9 and 10.

The variation in model performance may be due to differences in algorithmic structure or input parameters utilized in their development. Despite these differences, all models demonstrate potential for solar radiation estimation in Umudike, with Models 9 and 10 showing the highest degree of precision and reliability. A more detailed statistical evaluation would help confirm the best-performing model, but based on visual comparison and alignment with measured data, Models 9 and 10 are currently the most promising for accurate solar radiation prediction in the region.

4.0 Conclusion

The study revealed pronounced seasonal variations in global solar radiation and associated meteorological parameters in Umudike, Nigeria. The monthly mean daily extraterrestrial radiation (Ho) ranged from 33.38 MJ m^{-2} day^{-1} in June to 37.73 MJ m^{-2} day^{-1} in March. Measured global solar radiation (Hm) was lowest in August at 2.65 MJ m^{-2} day^{-1} and highest in May at 6.35 MJ m^{-2} day^{-1}, while the predicted values (Hp) followed a similar pattern, ranging from 2.75 MJ m^{-2} day^{-1} in August to 6.31 MJ m^{-2} day^{-1} in May. The clearness index (K), which indicates atmospheric transparency, reached a maximum of 0.18 in May and a minimum of 0.07 in August. The fraction of sunshine (ϴ) was highest in December at 0.47 and lowest in August at 0.18, reflecting increased cloud cover during the rainy season. Maximum air temperatures (Tmax) peaked in February at 34.1°C and declined to 28.7°C in August, while minimum temperatures (Tmin) ranged between 21.05°C in January and 23.50°C in April. August recorded the highest rainfall with 312.63 mm, and July had the highest relative humidity of 87.15%. The close agreement between predicted and observed radiation values demonstrates the reliability of the empirical models used.

The findings confirm that solar radiation in Umudike is strongly influenced by seasonal weather patterns, particularly rainfall, humidity, and cloud cover. Solar radiation availability is significantly reduced during the peak rainy season from July to September and enhanced during the dry months of November to May, when atmospheric clarity and sunshine duration are optimal. The strong correlation between solar radiation and sunshine hours, along with the consistency of measured and predicted data, validates the use of empirical methods for estimating solar energy potential in the region.

It is therefore recommended that solar energy systems in Umudike and similar tropical locations be optimized for installation and energy capture during the dry season when solar radiation is highest. Policymakers and energy planners should take seasonal radiation patterns into account when designing and implementing solar-based energy solutions.

Further studies are encouraged to refine the existing models by incorporating longer and more diverse datasets, as well as to investigate the long-term effects of climate variability on solar radiation. Public awareness and training initiatives should be implemented to educate stakeholders on the seasonal behavior of solar energy resources, and similar studies should be extended to other regions for broader application in energy planning.

5.0 References

Abdulkarim, S. D., Abdulkadir, A., Abbas, F. U., Gambo, A. M., Maira, S. M. B. & Mafola, S. (2024). Prediction of Monthly Mean Surface Air Temperature Using SARIMA in Jos North, Plateau State, Nigeria. *BIMA JOURNAL OF SCIENCE AND TECHNOLOGY (2536-6041)*, *8*(1B), 358-366. https://doi.org/10.56892/bima.v8i1B.646

Adedoja, O. S., Ayantunji, B. G., Saleh, U. A. & Jatto, S. S. (2015). Diurnal and seasonal variation of global solar radiation at Anyigba, North-Central Nigeria. *International Journal of Engineering Science and Innovative Technology (IJESIT)*, 4(4): 140-148. https://www.researchgate.net/publication/337022121.

Akpabio L. E, & Etuk S. E (2003). Relationship between solar radiation and sunshine duration for Onne Nigeria.,Turkish J. Phys. 27: 161 - 167.

Almorox, J., Benito, M., & Hontoria, C. (2005). Estimating of Monthly Angstrom – Prescott equation coefficients from measured daily data in Toledo, Spain. Renewable Energy J., 30, pp. 931 - 936.

Augustine, C. & Nnabuchi, M. N. (2010). Analysis of some meteorological data for some selected cities in the Eastern and Southern Zone of Nigeria. *African Journal of Environmental Science and Technology*, 4, 2, pp. 92–99.

Balling, R. C. & Roy, S. (2005). Analysis of spatial patterns underlying the linkage between solar irradiance and near-surface air temperatures. *Geophysical Research Letters*, 32, 11, L11702. https://doi.org/10.1029/2005GL022444 ADS2

Che, H. Z, Shi, G. Y., Zhang, X. Y, Zhao, J. Q. & Li Y (2007). Analysis of sky condition using 40 years records of solar radiation data in China. Theoretical and applied climatology 89, pp. 83 - 94.

Chukwuloka, E. H., Nwosu, A. O. & Ude, I. O. (2023). Air temperature time series modelling and prediction using neural network and SARIMA model. *Journal of the Nigerian Statistical Association*, 35, 2, pp. 1-8.

Climate Data (2025). Enugu weather in February. Retrieved from https://en.climate-data.org/africa/nigeria/enugu-350/r/february-2/ on 15th April, 2025.

Duffie, J.A. and Beckman, W.A. (1991) *Solar engineering of thermal processing*, 2nd ed. Madison: John Wiley &Sons, Inc., 1991.

El-Sebaii, A. A. and Trabea, A. A. (2005). Estimation of horizontal diffuse solar radiation in Egypt. *Energy Conversion and Management*, 44, 15, pp. 2471–2482 . doi: 10.1016/S0196-8904(03)00004-9

Gleisner, H. and Thejll, P. (2003). Patterns of tropospheric response to solar variability. *Geophysical Research Letters*, 30, 13, pp. 1-12. doi: 10.1029/2003GL017129.

Halouani M, Nguyen C. T, Vo Ngoc D (1993). Calculation of monthly average global solar radiation on horizontal surfaces using Daily Hours of Bright Sunshine, Solar energy 50, pp. 247-255.

Igbal M (1983). *An introduction to solar radiation*. Academy press. New york. pp. 6-51.

Meehl, G. A., Warren, M. W., Wigley, T. M. L. & Arblaster, J. M. (2003). Solar and greenhouse gas forcing and climate response in the twentieth century. *Journal of Climate*, 16, 3, pp. 26–444. doi: 10.1175/1520-0442(2003)016<0426: SAGGFA>2.0.CO;2

Nwokoye, A.O.C. (2006).Solar *Energy Technology; Other Alternative Energy Resources and Environmental Issues*; Rex Charles and Patrick Ltd, Nimo, Anambra State, Nigeria pp1-404.

Ododo, J. C., Sulaiman, A.T., Ogbu, F.A., Aidan, J. & Yuguda, M.M. (1995). The importance of maximum air temperature in the parameterisation of solar radiation in Nigeria. *Renewable Energy*, 6, 7, pp. 1-10. doi: 10.1016/0960-1481(94)00097-P

Soneye, O. O., Ayoola, M. A., Ajao, I. A. & Jegede, O. O. (2019). Diurnal and seasonal variations of the incoming solar radiation flux at a tropical station, Ile-Ife, Nigeria. *Heliyon*, 16;5(5):e01673. doi: 10.1016/j.heliyon.2019.e01673.

Stanhill, G., & S. Cohen, (2001): Global dimming: A review of the evidence for a widespread and significant reduction in global radiation with discussion of its probable causes and possible agricultural consequences. *Agricultural and Forest Meteorology*, 107, pp. 255-278.

Declaration

Consent for publication

Not applicable

Availability of data

Data shall be made available on demand.

Competing interests

The authors declared no conflict of interest

Ethical Consideration

Not applicable

Funding

There is no source of external funding.

Authors' contributions

All components of thr work were carried out by the authors